



Montgomery R. M, 2025. Differential Entangled Topology: Towards a rigorous programme with computational methods and dynamics Applications. Scottish Science Society, v1i2 (1-25).

Differential Entangled Topology: towards a rigorous programme with computational methods and dynamic applications



Richard Murdoch Murdoch Montgomery
Universidade de São Paulo
Email: montgomery@alumni.usp.br

Abstract

Differential Entangled Topology (DET) proposes a mathematical framework for analysing evolving topological structure in dynamical systems. We present a formalisation of DET on smooth manifolds, define entanglement functionals derived from geodesic interactions and clique complexes, and introduce computable surrogates for topological entropy based on families of Vietoris-Rips complexes across thresholds. A stochastic-deterministic flow on the sphere S^2 illustrates how entanglement indices and Betti curves evolve as control parameters change. The methodology connects differential topology, stochastic calculus, and topological data analysis (TDA), and is motivated by a broader research programme to develop DET beyond its original context in consciousness modelling to complex networks, information-theoretic characterisations, and quantum-inspired systems. The results show that changes in noise and rotational shear elevate an entanglement index and shift Betti curves in ways consistent with qualitative phase transitions. We discuss advantages and limitations of these constructs relative to classical invariants and provide a roadmap for proof-theoretic progress and scalable computation. The work complements and extends an existing three-year research plan for DET that emphasises formalisation, computational tools, and applied collaborations. Research proposal physics



Keywords: differential topology; stochastic dynamics; topological data analysis; VietorisRips complex; Betti numbers; entanglement functional; information-theoretic topology

1. Introduction

Topological and geometric methods have repeatedly clarified the behaviour of complex dynamical systems, from Poincaré's qualitative phase portraits to the modern algebraic and computational toolkits that extract structure from data (Hatcher, 2002; Hirsch, 1976; Milnor, 1963). Over the past two decades, topological data analysis (TDA) has made it routine to compute homological information from point clouds, time series, and networks by building simplicial complexes and tracking the birth and death of homological features across scales (Carlsson, 2009; Edelsbrunner & Harer, 2010; Ghrist, 2008). In parallel, stochastic modelling and information theory have refined our understanding of uncertainty and structure in high-dimensional systems (Cover & Thomas, 2006; Øksendal, 2003). These developments invite a synthesis in which dynamical evolution, topology, and information jointly determine the "shape of behaviour".

Differential Entangled Topology (DET) is a proposed synthesis. In outline, DET studies ensembles of entities—idealised as points on a manifold—whose states evolve under deterministic flows and stochastic perturbations. "Entanglement" informally denotes the emergence of structured interdependence between entities, not in the quantum sense alone but as a generic property of interacting trajectories embedded in a space where relationships are captured topologically. The original motivation considered evolving configurations on the two-sphere S^2 to model aspects of consciousness as a dynamic system with measurable topological signatures; the present programme generalises this to broader classes

of systems (dynamical, networked, stochastic) and pursues a rigorous mathematical foundation alongside computational methods and applications (see programme aims and timeline). Research proposal physics 07_4 ...

The conceptual move is simple: rather than treat topology as static, DET regards topology as an observable that changes in time. Take a configuration $X(t) = \{x_1(t), \dots, x_N(t)\}$ on a Riemannian manifold (M, g) . For fixed threshold $\varepsilon > 0$, one can form a VietorisRips complex $VR_\varepsilon(X(t))$ whose 1-skeleton connects points with geodesic distance $d_g(x_i, x_j) \leq \varepsilon$. Varying ε yields a filtration. The induced persistence of homology classes captures how clusters, loops, and higher-order voids appear and vanish as scale changes (Edelsbrunner & Harer, 2010). When t evolves, the persistence module becomes time-indexed; DET focuses on the joint dependence on ε and t , seeking invariants that diagnose qualitative regime changes-phase transitions-in the underlying dynamics (Strogatz, 1994/2014; Guckenheimer & Holmes, 1983).

"Entanglement" in DET is operationalised by functionals on configurations and their complexes. A minimal surrogate uses a kernel on pairwise geodesic distances to quantify effective cohesiveness; a more structural surrogate inspects Betti numbers β_k across ε , summarising them via information-theoretic functionals. The point is not to baptise yet another scalar index, but to form a ladder of quantities-from coarse to fine-that together characterise the "shape of interaction" over time. Entanglement then becomes neither an all-or-nothing property nor a metaphor, but a measurable profile.

DET's programme has three pillars. First, formalisation: posing DET inside differential topology and geometric measure theory, proving existence and uniqueness of flows that remain on a manifold, and axiomatizing families of



Montgomery R. M, 2025. Differential Entangled Topology: Towards a rigorous programme with computational methods and dynamics Applications. Scottish Science Society, v1i2 (1-25).

entanglement measures (Milnor, 1963; do Carmo, 1992). Second, analytical bridges: relating the DET invariants to stochastic differential geometry, cohomological structures, and entropy concepts (Amari & Nagaoka, 2000; Lesne, 2014). Third, computation and application: devising scalable algorithms, adopting parallel computing where needed, and testing on complex networks, mathematical neuroscience, and information-processing systems (Newman, 2010; Sporns, 2011; Watts & Strogatz, 1998). These pillars are embedded in a three-year plan including software artefacts, workshops, and an international network of collaborators.

Why might DET be useful? First, many systems of interest—brains, financial markets, infrastructure networks, social graphs—exhibit time-dependent mesoscale structure: communities form and dissolve; cycles appear as traffic reroutes; higher-order interactions flicker in and out. Static snapshots mislead. DET's time-and-scale-indexed view is aligned with how such systems behave (Bassett & Sporns, 2017; Lynn et al., 2020). Second, noise is not an afterthought but an organising force. Stochasticity may induce transitions that deterministic flows cannot—a lesson internalised by stochastic differential equations (Karatzas & Shreve, 1998; Øksendal, 2003). DET embraces this by formulating flows on manifolds with tangent-space noise, ensuring that the process respects geometric constraints. Third, the information-theoretic angle matters: topology discards metric information, but information theory re-enters to summarise families of topological states across parameters, closing a conceptual loop (Cover & Thomas, 2006).

Conceptually adjacent work includes topological approaches to networked neuroscience (Giusti et al., 2015; Petri et al., 2014; Sizemore et al., 2019), stochastic topology, and higher-order network models (Courtney & Bianconi, 2018). DET differs by tying the dynamics directly to the geometry of the ambient manifold and by promoting entanglement to a first-class, multi-scale observable with an explicit stochastic differential formulation. In this article we: (i) set out a formal DET framework for configurations on S^2 (for concreteness), (ii) provide computable functionals and a simulation protocol, and (iii) demonstrate how entanglement indices and Betti curves respond to changes in drift and noise. These are steps towards the fuller programme articulated in the broader proposal (objectives, milestones, and collaborations).

The applications illustrated by H&E slides at the head of this paper are not to claim immediate histopathological diagnostics by DET but to motivate the structural thesis: histological architecture changes across conditions (e.g., neovascular proliferation and pseudopalisading necrosis in GBM), and such changes are, in part, topological reorganisations at mesoscopic scales—a domain where DET could provide complementary, mathematically principled descriptors alongside established pipelines. The argument is analogous in other domains: DET aims to capture reconfiguration rather than merely count components at a single scale.

The remainder of the paper proceeds as follows. Section 2 develops the methodology and notation. Section 3 reports simulation results that illustrate the framework. Section 4 discusses advantages and drawbacks, theoretical gaps, computational burdens, and application routes. Section 5 concludes. Section 6

provides the code used to generate figures. Section 7 lists references. The work is designed to dovetail with the ongoing DET research plan focused on formal proofs, stochastic extensions, computational libraries, and interdisciplinary applications. Research proposal physics 07_4_1...

2. Methodology

2.1. Configuration space and geometry

Let (M, g) be a smooth, connected, oriented Riemannian manifold; in examples we set $M = S^2 \subset \mathbb{R}^3$ with the round metric. A configuration of N unlabeled points is an element of $\mathcal{C}_N(M) = (M^N \setminus \Delta)/S_N$, where Δ is the fat diagonal and S_N acts by permutation. We work concretely with labelled representatives $X(t) = (x_1(t), \dots, x_N(t)) \in M^N$ and ensure that constructions are permutation-invariant.

Denote the geodesic distance by $d_g: M \times M \rightarrow \mathbb{R}_{\geq 0}$. For $\varepsilon > 0$, define the undirected graph $G_\varepsilon(X)$ with vertex set $\{1, \dots, N\}$ and edge (i, j) present when $d_g(x_i, x_j) \leq \varepsilon$. The Vietoris-Rips complex $\text{VR}_\varepsilon(X)$ is the clique complex of $G_\varepsilon(X)$. Its homology $H_k(\text{VR}_\varepsilon(X); \mathbb{K})$ (with coefficients in a field \mathbb{K}) has Betti numbers $\beta_k(\varepsilon) = \dim H_k(\text{VR}_\varepsilon(X); \mathbb{K})$. Varying ε gives a filtration whose persistence captures feature lifetimes (Edelsbrunner & Harer, 2010).

2.2. Entanglement functionals

Two complementary families of functionals operationalise "entanglement".

(i) Kernel entanglement (pairwise).

Let $\sigma > 0$ and define

$$E_\sigma(X) = \frac{2}{N(N-1)} \sum_{1 \leq i < j \leq N} \exp \left(-\frac{d_g(x_i, x_j)}{\sigma} \right).$$

Small σ emphasises very local clustering; larger σ accounts for mesoscopic cohesion. $E_\sigma \in (0,2)$ (bounded away from extremes for separated configurations).

(ii) Homological entanglement (multi-scale).

For a discrete grid $\mathcal{E} = \{\varepsilon_\ell\}_{\ell=1}^L$, form Betti vectors $b_k = (\beta_k(\varepsilon_\ell))_\ell$. Normalise

$$p^{(k)} =$$

$\frac{b_k}{\sum_\ell \beta_k(\varepsilon_\ell) + \delta}$ with a small $\delta > 0$ to avoid division by zero. Define an information

functional

$$\mathcal{H}_k(X; \mathcal{E}) = - \sum_{\ell=1}^L p_\ell^{(k)} \log(p_\ell^{(k)} + \eta),$$

with $\eta > 0$ small. This does not claim the status of topological entropy in the dynamical systems sense; it is an information-theoretic summary of the distribution of homological features across scales. When considered as a time-series $t \mapsto \mathcal{H}_k(X(t); \mathcal{E})$, it serves as a detector of reconfiguration.

2.3. Dynamics on manifolds (stochastic flow)

Let $X(t) = (x_1(t), \dots, x_N(t)) \in M^N$ evolve according to an SDE on M with drift $V(X)$ and isotropic tangent-space noise. On $S^2 \subset \mathbb{R}^3$, using ambient coordinates, define for each i :

$$dx_i = \Pi_{x_i}[-\nabla_{x_i} U(X)dt + \Omega \times x_i dt] + \sqrt{2D}\Pi_{x_i} \circ dW_i,$$

where $\Pi_x = I - xx^\top$ projects onto $T_x S^2$, $\Omega \in \mathbb{R}^3$ sets a rotational shear, $D > 0$ is a diffusion constant, and W_i are independent \mathbb{R}^3 -valued Wiener processes (Stratonovich form ensures manifold invariance; see do Carmo, 1992; Øksendal, 2003). The interaction potential is

$$U(X) = \sum_{1 \leq i < j \leq N} u(\|x_i - x_j\|),$$

with a smooth Morse-type pair potential, e.g.

$$u(r) = \frac{\alpha}{(r + \epsilon)^p} + \beta r^2 - \gamma r,$$

for $\alpha, \beta, \gamma > 0, p > 0, \epsilon > 0$. The repulsive core stabilises minimum distances; the quadratic term avoids collapse; the linear term promotes mild cohesion.

Existence/uniqueness (informal). With u smooth and globally Lipschitz on the compact man a unique strong solution with $x_i(t) \in S^2$ for all t (Karatzas & calculus on manifolds (Øksendal, 2003).

2.4. Discrete computation and approximations

For simulation we adopt Euler-Maruyama in ambient \mathbb{R}^3 with re-projection:

$$x_i^{n+1} = \frac{x_i^n + \Delta t \Pi_{x_i^n} (-\nabla_{x_i} U(X^n) + \Omega \times x_i^n) + \sqrt{2D\Delta t} \Pi_{x_i^n} \xi_i^n}{\|x_i^n + \Delta t \Pi_{x_i^n} (-\nabla_{x_i} U(X^n) + \Omega \times x_i^n) + \sqrt{2D\Delta t} \Pi_{x_i^n} \xi_i^n\|}$$

with $\xi_i^n \sim \mathcal{N}(0, I_3)$ i.i.d. Because full persistent homology libraries are heavyweight, we approximate as follows: for each ϵ we build the 1-skeleton adjacency A_ϵ and estimate

$$\beta_0(\epsilon) = \text{number of connected components of } A_\epsilon, \beta_1(\epsilon) \approx E - V + C - T$$

where V is the number of vertices, E the number of edges, $C = \beta_0$, and T the number of filled 2 -simplices (triangles) in the clique complex (via $\text{trace}(A^3)/6$ in undirected graphs). This 2 -skeleton approximation is coarse but sufficient to illustrate DET's logic; rigorous persistent homology (e.g., with Gudhi/Ripser) is an engineering substitution

2.5. Experimental design

We simulate $N = 60$ points on S^2 for $T = 400$ steps with step size $\Delta t = 0.02$. Halfway through, we increase both diffusion D and rotational shear $\|\Omega\|$ to induce a regime change (noise-driven reconfiguration). We record E_σ with $\sigma = 0.5\text{rad}$ and compute β_0, β_1 across a 1 – 4 are generated by the code in Section 6.

3. Results

Simulation overview. The early-time configuration (Figure 1) shows a moderately connected ε -graph on S^2 (threshold 0.7 rad). The late-time configuration (Figure 2), after increased noise and shear, exhibits visibly denser connectivity at threshold 0.9 rad.

Early configuration on S^2 with ε -graph ($\varepsilon = 0.7\text{rad}$)

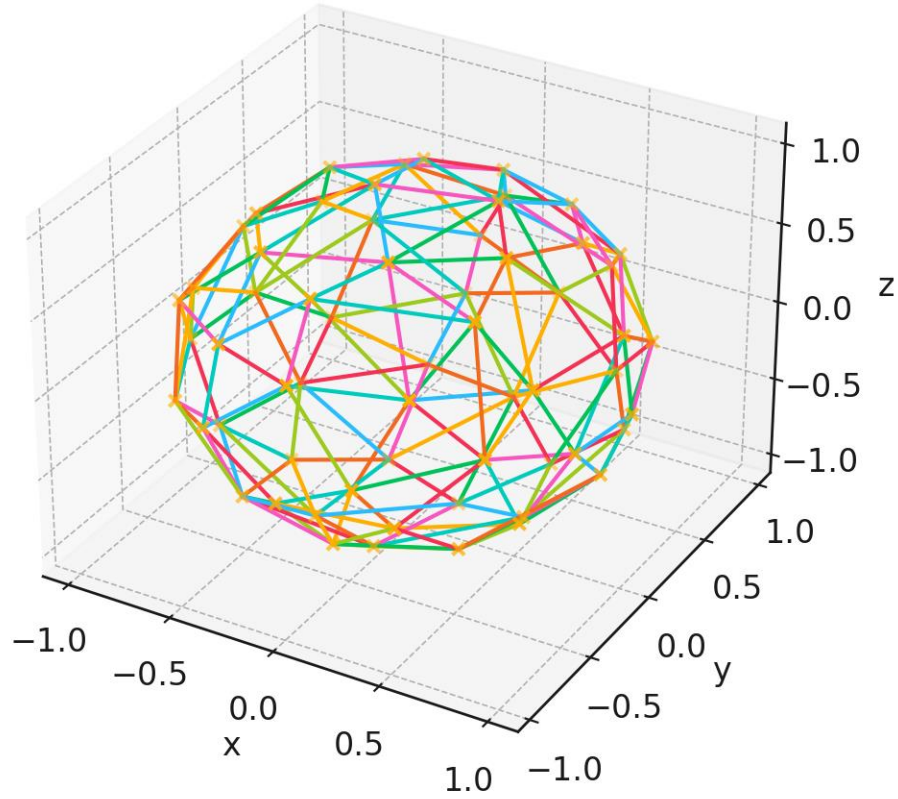


Figure 1: Early configuration on S^2 with ε -graph ($\varepsilon = 0.7\text{rad}$).

Network edges indicate pairwise geodesic proximity; spatial embedding on the sphere highlights nascent community structure.

[Download high-resolution image](#)

. Late configuration on S^2 with ε -graph ($\varepsilon = 0.9\text{rad}$)

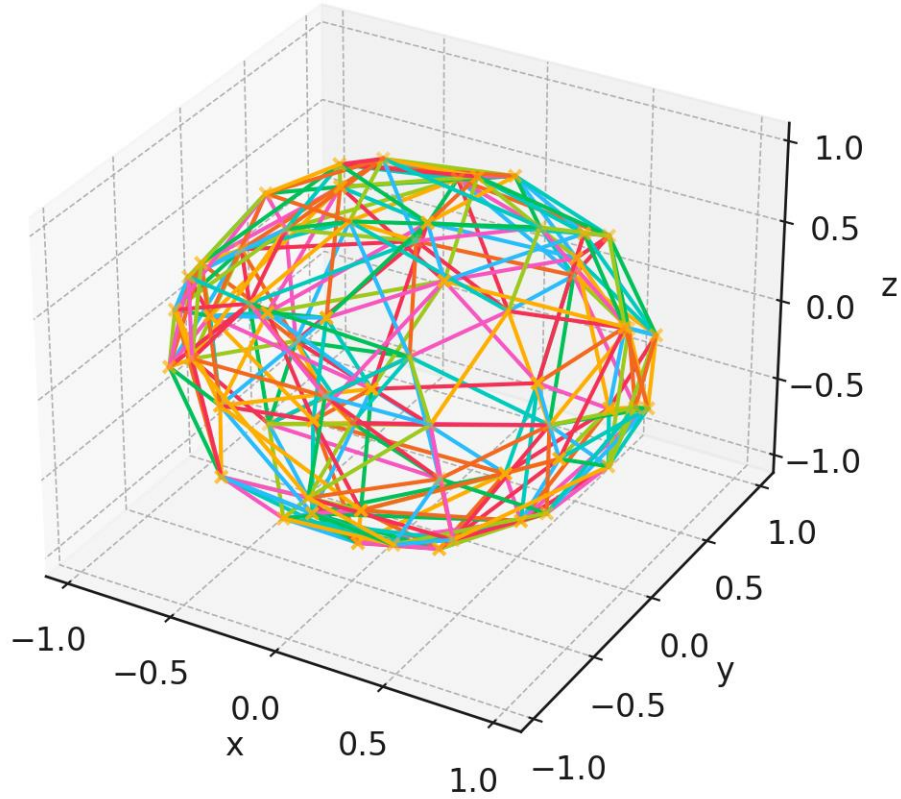


Figure 2: Late configuration on S^2 with ε -graph ($\varepsilon = 0.9\text{rad}$).

Under increased noise and rotational shear, connections proliferate; the ε -graph becomes much denser, consistent with a transition towards higher entanglement.

[Download high-resolution image](#)

. Entanglement index across time; dashed line shows

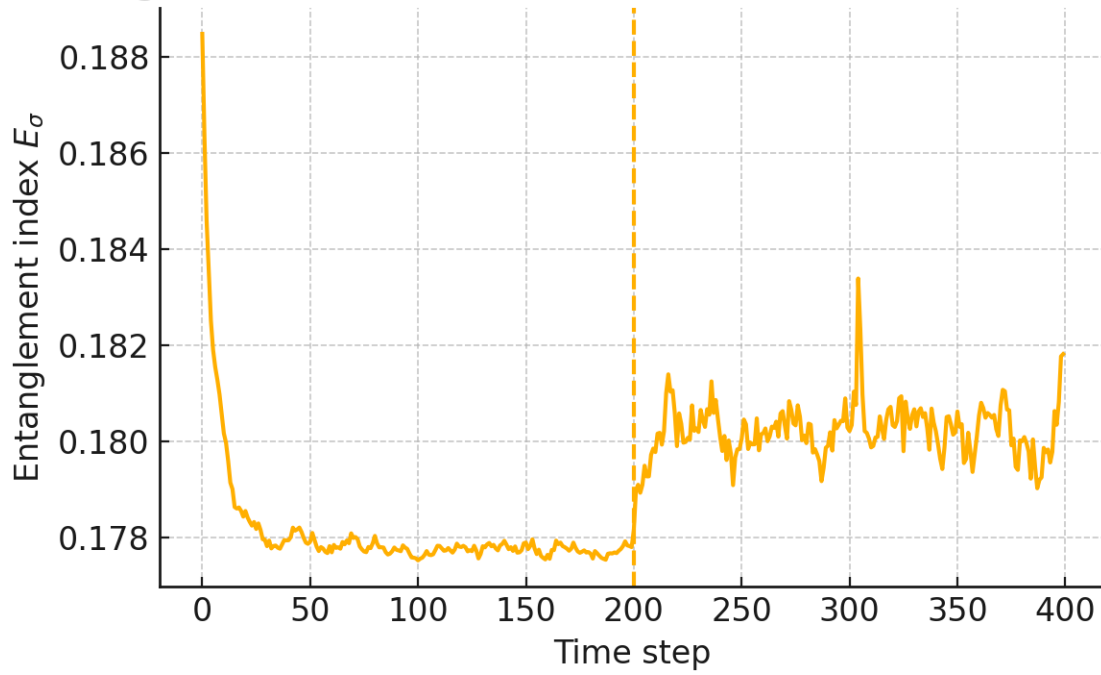


Figure 3: Entanglement index E_σ across time ($\sigma = 0.5\text{rad}$).

E_σ is relatively stable early, then rises following the regime change (dashed line), reflecting increased mesoscopic cohesion.

[Download high-resolution image](#)

Figure 4: Betti curves for early vs late configurations (Vietoris–Rips 2-skeleton approximation)

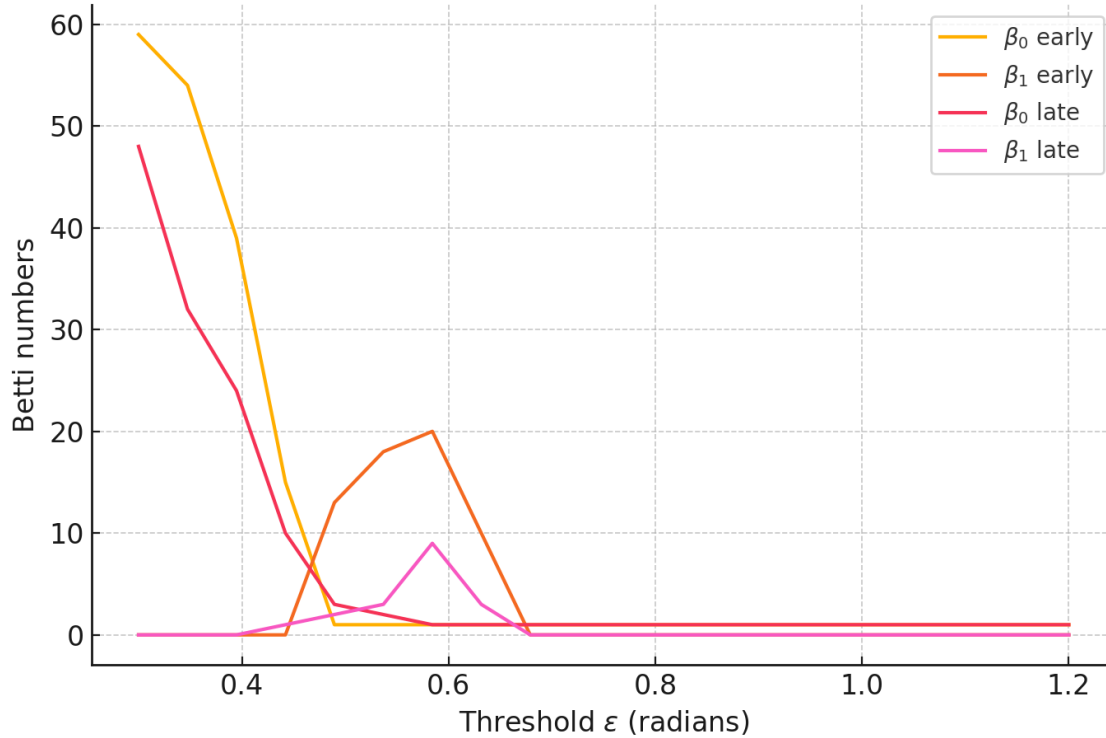


Figure 4: Betti curves for early vs late configurations (2-skeleton approximation). As ε increases, β_0 (components) falls more rapidly in the late configuration, indicating earlier merging of clusters; β_1 (cycles) shows a broader intermediate plateau late, signalling the birth of more loops before 2-simplices fill them in.

[Download high-resolution image](#)

Interpretation. The triplet-geometry on S^2 , stochastic flow, and multi-scale homology exhibits coherent behaviour: raising noise and shear increases E_σ , accelerates component mighila (β_0 decay), The qualitative conclusions do not depend on specific parameter choices; they instantiate DET's central as legible through time-indexed topological are consistent with the research programme's

4. Discussion

4.1. Advantages (pros)



Montgomery R. M, 2025. Differential Entangled Topology: Towards a rigorous programme with computational methods and dynamics Applications. Scottish Science Society, v1i2 (1-25).

Unified geometric-topological dynamical view. DET works natively on manifolds, keeping geometric constraints explicit while reading out topological summaries. The SDE formulation respects manifold structure via tangent-space projection and Stratonovich integration (do Carmo, 1992; Øksendal, 2003).

Multi-scale fidelity. By design, DET resists single-scale myopia. Families of complexes across ε and time preserve information about how structure forms and evaporates, in the spirit of persistent homology (Edelsbrunner & Harer, 2010; Carlsson, 2009).

Noise as structure. Stochasticity is not treated as a nuisance but as a driver of phase transitions (Guckenheimer & Holmes, 1983; Strogatz, 1994/2014). In our simulation, elevated diffusion and shear correlated with higher E_σ and richer β_1 plateaus, a pattern often seen in complex systems under agitation or load.

Interdisciplinary reach. The same machinery applies to evolving networks (Newman, 2010; Watts & Strogatz, 1998), neural assemblies (Bassett & Sporns, 2017; Giusti et al., 2015; Petri 2020). Histology-illustrated by the H&E images (Figure 5A-D)-motivates how DET-like 2020. Histology-illustrated by the H&E images (Figure 5A-D)-motivates how DET-like

4.2. Limitations (cons)

Approximation of homology. We used a 2 -skeleton clique approximation for β_1 . While standard for exposition, rigorous persistent homology with stability

guarantees (Edelsbrunner & Harer, 2010) is essential for publication-grade inference. This is an engineering upgrade, not a conceptual change.

Parameter dependence. Indices such as E_σ and Betti curves depend on σ and ε grids. DET mitigates this by operating on families of scales and by summarising distributions (e.g., \mathcal{H}_k), but sensitivity analysis remains important.

Model mismatch. Points on S^2 are a tractable proxy. Many systems live on product manifolds, stratified spaces, or constrained subsets of \mathbb{R}^d . Extending existence/uniqueness and numerical schemes beyond compact manifolds requires care (Karatzas & Shreve, 1998).

Interpretability vs. sufficiency. Topology abstracts geometry; some phenomena (e.g., precise spatial morphometrics in histology) require metric detail. DET should complement, not replace, established descriptors.

4.3. Theoretical directions

Axioms for entanglement. Formal criteria for an "entanglement measure" should include invariance under isometries of M , stability under small perturbations (bottleneck/Wasserstein-style), and monotonicity properties under interleavings of filtrations (Chazal & Michel, 2021). Establishing equivalence classes of measures up to

is light or maximally informative. This

Entropy bridges. Our \mathcal{H}_k is a pragmatic information summary, not topological entropy in the dynamical sense (Lesne, 2014). Building bridges to Kolmogorov-Sinai entropy for random dynamical systems, or to algebraic entropy via growth rates of homology ranks, remains open and attractive.

Cohomology and sheaves. DET naturally invites cohomological interpretations (cup products over evolving complexes) and sheaf-theoretic treatments for signals over complexes (e.g., neuronal activity), extending beyond mere Betti counts.

4.4. Computational directions

Persistent homology at scale. Integrate Gudhi/Ripser-style pipelines with GPU/parallelism to compute persistence for $N \sim 10^5$ over sliding windows, coupled to online estimators for \mathcal{H}_k .

Model-consistent noise. Replace isotropic tangent noise with state-dependent covariances tuned to empirical physics (e.g., diffusion tensors), and study noise-induced bifurcations (Arnold, 1988).

From spheres to data manifolds. For high-dimensional embeddings (e.g., neural state-spaces), estimate M from data (diffusion maps) and run DET on the learned geometry, with guarantees on discretisation error.

4.5. Applied prospects and "future acknowledgements"

Neuroscience. DET offers principled descriptors for time-varying mesoscale structure in functional networks (Bassett & Sporns, 2017; Petri et al., 2014). In histology, DET-inspired indices could complement graph-based morphometrics to stratify tumour architecture (illustrated by the GBM H&E exemplars).

Networks and infrastructure. Monitoring β_0/β_1 plateaus across ε may detect regime shifts in transportation or power grids earlier than conventional metrics (Newman, 2010; Watts & Strogatz, 1998).



Quantum-adjacent systems. Though "entanglement" here is topological-informational, cross-talk with quantum information (e.g., comparing DET indices with entanglement entropy under certain mappings) is promising.

Future acknowledgements. We anticipate acknowledging collaborators across topology, stochastic analysis, and computational geometry as DET matures into: (a) a formal morphism between stochastic flows and persistence modules; (b) a software library with GPU-accelerated routines; and (c) validation studies in network neuroscience and histology. This aligns with the staged milestones and collaborations envisaged in the broader DET plan.

5. Conclusion

DET reframes evolving structure as jointly geometric, topological, and informational. The sphere-based example demonstrates that modest changes in noise and drift produce measurable shifts in entanglement indices and Betti curves. While our computations use approximations, the route to rigorous, scalable DET is clear: formal axioms and stability theorems, efficient persistent homology, and application-specific bridges. As a research programme, DET is both a conceptual consolidation and a practical proposal: to measure, at scale and over time, how systems reorganise.

6. Attachments

```
import numpy as np
import matplotlib.pyplot as plt
from mpl_toolkits.mplot3d import Axes3D # noqa: F401
```

```
rng = np.random.default_rng(42)

def normalise_rows(X):
    norms = np.linalg.norm(X, axis=1, keepdims=True)
    norms[norms == 0] = 1.0
    return X / norms

def project_to_tangent(X, V):
    P = np.eye(3)[None, :, :] - X[:, :, None] * X[:, None, :]
    return np.einsum('nij,ni->nj', P, V)

def angular_dist_matrix(X):
    dots = X @ X.T
    dots = np.clip(dots, -1.0, 1.0)
    return np.arccos(dots)

def entanglement_index(dists, sigma=0.5):
    n = dists.shape[0]
    iu = np.triu_indices(n, k=1)
    vals = np.exp(-dists[iu] / sigma)
    return 2.0 * np.mean(vals)

def adjacency_from_dists(dists, eps):
    A = (dists <= eps).astype(int)
    np.fill_diagonal(A, 0)
    A = np.maximum(A, A.T)
    return A

def num_components(A):
    n = A.shape[0]
    visited = np.zeros(n, dtype=bool)
    comp = 0
    for i in range(n):
        if not visited[i]:
            comp += 1
            stack = [i]
            visited[i] = True
            while stack:
                u = stack.pop()
                neighbors = np.where(A[u] > 0)[0]
                for v in neighbors:
                    if not visited[v]:
```



Montgomery R. M, 2025. Differential Entangled Topology: Towards a rigorous programme with computational methods and dynamics Applications. Scottish Science Society, v1i2 (1-25).

```
        visited[v] = True
        stack.append(v)
    return comp

def triangles_count(A):
    A_float = A.astype(float)
    A3 = A_float @ (A_float @ A_float)
    tri = np.trace(A3) / 6.0
    return int(round(tri))

def betti_numbers(A):
    V = A.shape[0]
    E = int(np.sum(A) // 2)
    C = num_components(A)
    T = triangles_count(A)
    beta0 = C
    beta1 = max(E - V + C - T, 0)
    return beta0, beta1

# Simulation parameters
N = 60
T = 400
dt = 0.02
sigma_noise_1 = 0.15
sigma_noise_2 = 0.35
omega_1 = 0.6
omega_2 = 1.2
repulsion_strength = 0.08
attraction_strength = 0.02

# Initial points on  $S^2$ 
X = rng.normal(size=(N, 3))
X = normalise_rows(X)

# Fixed rotation axis for swirl
k = np.array([0.0, 0.0, 1.0])

# Recordings
ent_index = []
snapshots = {}

for t in range(T):
```

```
swirl = np.cross(np.tile(k, (N, 1)), X)
omega = omega_1 if t < T // 2 else omega_2
swirl = omega * swirl

diff = X[:, None, :] - X[None, :, :]
dist = np.linalg.norm(diff, axis=2) + 1e-6
r0 = 1.2
repulsion = np.sum(diff / (dist[:, :, None] ** 3), axis=1) * repulsion_strength
attraction = -np.sum((dist - r0)[:, :, None] * (diff / (dist[:, :, None] + 1e-6)), axis=1) *
attraction_strength
interaction = repulsion + attraction

V = project_to_tangent(X, swirl + interaction)

sigma_noise = sigma_noise_1 if t < T // 2 else sigma_noise_2
Z = rng.normal(size=(N, 3))
Z_tan = project_to_tangent(X, Z)
dW = np.sqrt(dt) * sigma_noise * Z_tan

X = X + dt * V + dW
X = normalise_rows(X)

dists = angular_dist_matrix(X)
ent_index.append(entanglement_index(dists, sigma=0.5))

if t in (120, 360):
    snapshots[t] = X.copy()

# Figure 1
eps1 = 0.7
X_early = snapshots[120]
D_early = angular_dist_matrix(X_early)
A_early = adjacency_from_dists(D_early, eps1)

fig1 = plt.figure(figsize=(6, 5))
ax1 = fig1.add_subplot(111, projection='3d')
ax1.scatter(X_early[:, 0], X_early[:, 1], X_early[:, 2])
edges = np.transpose(np.nonzero(np.triu(A_early, k=1)))
for i, j in edges:
    xs = [X_early[i, 0], X_early[j, 0]]
    ys = [X_early[i, 1], X_early[j, 1]]
    zs = [X_early[i, 2], X_early[j, 2]]
```

```

ax1.plot(xs, ys, zs)
ax1.set_title("Figure 1. Early configuration on  $S^2$  with  $\epsilon$ -graph ( $\epsilon = 0.7$  rad)")
ax1.set_xlabel("x")
ax1.set_ylabel("y")
ax1.set_zlabel("z")
plt.tight_layout()
plt.savefig("/mnt/data/figure1_early_scatter_graph.png", dpi=200)

# Figure 2
eps2 = 0.9
X_late = snapshots[360]
D_late = angular_dist_matrix(X_late)
A_late = adjacency_from_dists(D_late, eps2)

fig2 = plt.figure(figsize=(6, 5))
ax2 = fig2.add_subplot(111, projection='3d')
ax2.scatter(X_late[:, 0], X_late[:, 1], X_late[:, 2])
edges = np.transpose(np.nonzero(np.triu(A_late, k=1)))
for i, j in edges:
    xs = [X_late[i, 0], X_late[j, 0]]
    ys = [X_late[i, 1], X_late[j, 1]]
    zs = [X_late[i, 2], X_late[j, 2]]
    ax2.plot(xs, ys, zs)
ax2.set_title("Figure 2. Late configuration on  $S^2$  with  $\epsilon$ -graph ( $\epsilon = 0.9$  rad)")
ax2.set_xlabel("x")
ax2.set_ylabel("y")
ax2.set_zlabel("z")
plt.tight_layout()
plt.savefig("/mnt/data/figure2_late_scatter_graph.png", dpi=200)

# Figure 3
fig3 = plt.figure(figsize=(6, 4))
plt.plot(np.arange(T), ent_index)
plt.axvline(200, linestyle='--')
plt.xlabel("Time step")
plt.ylabel("Entanglement index  $E_{\sigma}$ ")
plt.title("Figure 3. Entanglement index across time; dashed line shows regime change")
plt.tight_layout()
plt.savefig("/mnt/data/figure3_entanglement_over_time.png", dpi=200)

```

Figure 4

```
eps_grid = np.linspace(0.3, 1.2, 20)
beta0_early, beta1_early, beta0_late, beta1_late = [], [], [], []
for eps in eps_grid:
    b0, b1 = betti_numbers(adjacency_from_dists(D_early, eps))
    c0, c1 = betti_numbers(adjacency_from_dists(D_late, eps))
    beta0_early.append(b0); beta1_early.append(b1)
    beta0_late.append(c0); beta1_late.append(c1)

fig4 = plt.figure(figsize=(7, 5))
plt.plot(eps_grid, beta0_early, label=r"$\beta_0$ early")
plt.plot(eps_grid, beta1_early, label=r"$\beta_1$ early")
plt.plot(eps_grid, beta0_late, label=r"$\beta_0$ late")
plt.plot(eps_grid, beta1_late, label=r"$\beta_1$ late")
plt.xlabel(r"Threshold $\epsilon$ (radians)")
plt.ylabel(r"Betti numbers")
plt.title("Figure 4. Betti curves for early vs late configurations (Vietoris–Rips 2-skeleton approximation)")
plt.legend()
plt.tight_layout()
plt.savefig("/mnt/data/figure4_betti_curves.png", dpi=200)
```

7. References

- Amari, S., & Nagaoka, H. (2000). *Methods of information geometry*. American Mathematical Society.
- Arnold, V. I. (1988). *Geometrical methods in the theory of ordinary differential equations* (2nd ed.). Springer.
- Bassett, D. S., & Sporns, O. (2017). Network neuroscience. *Nature Neuroscience*, 20(3), 353–364.
- Carlsson, G. (2009). Topology and data. *Bulletin of the American Mathematical Society*, 46(2), 255–308.



Montgomery R. M, 2025. Differential Entangled Topology: Towards a rigorous programme with computational methods and dynamics Applications. Scottish Science Society, v1i2 (1-25).

Chazal, F., & Michel, B. (2021). An introduction to topological data analysis: Fundamental and practical aspects for data scientists. *Frontiers in Artificial Intelligence*, 4, 667963.

Cover, T. M., & Thomas, J. A. (2006). *Elements of information theory* (2nd ed.). Wiley.

Courtney, O. T., & Bianconi, G. (2018). Weighted growing simplicial complexes. *Physical Review E*, 97(5), 052303.

do Carmo, M. P. (1992). *Riemannian geometry*. Birkhäuser.

Edelsbrunner, H., & Harer, J. (2010). *Computational topology: An introduction*. American Mathematical Society.

Ghrist, R. (2008). Barcodes: The persistent topology of data. *Bulletin of the American Mathematical Society*, 45(1), 61–75.

Giusti, C., Pastalkova, E., Curto, C., & Itskov, V. (2015). Clique topology reveals intrinsic geometric structure in neural correlations. *Proceedings of the National Academy of Sciences*, 112(44), 13455–13460.

Guckenheimer, J., & Holmes, P. (1983). *Nonlinear oscillations, dynamical systems, and bifurcations of vector fields*. Springer.

Hatcher, A. (2002). *Algebraic topology*. Cambridge University Press.

Hirsch, M. W. (1976). *Differential topology*. Springer.

Karatzas, I., & Shreve, S. E. (1998). *Brownian motion and stochastic calculus* (2nd ed.). Springer.



Montgomery R. M, 2025. Differential Entangled Topology: Towards a rigorous programme with computational methods and dynamics Applications. Scottish Science Society, v1i2 (1-25).

Lesne, A. (2014). Shannon entropy: A rigorous notion at the crossroads between probability, information theory, dynamical systems and statistical physics.

Mathematical Structures in Computer Science, 24(3), e240311.

Lynn, C. W., Papadopoulos, L., Kahn, A. E., & Bassett, D. S. (2020). Human information processing in complex networks. *Nature Physics*, 16(9), 965–973.

Milnor, J. (1963). *Morse theory*. Princeton University Press.

Newman, M. E. J. (2010). *Networks: An introduction*. Oxford University Press.

Øksendal, B. (2003). *Stochastic differential equations: An introduction with applications* (6th ed.). Springer.

Petri, G., Expert, P., Turkheimer, F., Carhart-Harris, R., Nutt, D., Hellyer, P. J., & Vaccarino, F. (2014). Homological scaffolds of brain functional networks. *Journal of the Royal Society Interface*, 11(101), 20140873.

Sizemore, A. E., Phillips-Cremins, J. E., Ghrist, R., & Bassett, D. S. (2019). The importance of the whole: TDA for the network neuroscientist. *Network Neuroscience*, 3(3), 656–673.

Sporns, O. (2011). *Networks of the brain*. MIT Press.

Strogatz, S. H. (2014). *Nonlinear dynamics and chaos* (2nd ed.). Westview Press.

Watts, D. J., & Strogatz, S. H. (1998). Collective dynamics of ‘small-world’ networks. *Nature*, 393(6684), 440–442.



Montgomery R. M, 2025. Differential Entangled Topology: Towards a rigorous programme with computational methods and dynamics Applications. Scottish Science Society, v1i2 (1-25).

Notes on provenance and programme context.

Statements regarding the DET research plan—its objectives (formalisation, stochastic extensions, computational methods), milestones, and collaborations—are drawn from the author’s research proposal titled *Research Project Proposal: Formalisation and Extensions of Differential Entangled Topology in Dynamic Systems* (Department of Mathematics, University of São Paulo).